β-decay study of the $T_z = -2$ proton-rich nucleus ^{20}Mg

L. J. Sun (孙立杰),[1] X. X. Xu (徐新星),[1,*] D. Q. Fang (方德清),[2,†] C. J. Lin (林承键),[1,3,‡] J. S. Wang (王建松),[4]
Z. H. Li (李智焕),[5] Y. T. Wang (王玉廷),[2] J. Li (李晶),[5] L. Yang (杨磊),[1] N. R. Ma (马南茹),[1] K. Wang (王康),[2]
H. L. Zang (臧宏亮),[5] H. W. Wang (王宏伟),[2] C. Li (李琛),[2] C. Z. Shi (施晨钟),[2] M. W. Nie (聂茂武),[2] X. F. Li (李秀芳),[2]
H. Li (李贺),[2] J. B. Ma (马军兵),[4] P. Ma (马朋),[4] S. L. Jin (金仕纶),[4] M. R. Huang (黄美容),[4] Z. Bai (白真),[4]
J. G. Wang (王建国),[4] F. Yang (杨峰),[1] H. M. Jia (贾会明),[1] H. Q. Zhang (张焕乔),[1] Z. H. Liu (刘祖华),[1] P. F. Bao (包鹏飞),[1]
D. X. Wang (王东玺),[1] Y. Y. Yang (杨彦云),[4] Y. J. Zhou (周远杰),[4] W. H. Ma (马维虎),[4] J. Chen (陈杰),[4] Y. G. Ma (马余刚),[2]
Y. H. Zhang (张玉虎),[4] X. H. Zhou (周小红),[4] H. S. Xu (徐瑚珊),[4] G. Q. Xiao (肖国青),[4] and W. L. Zhan (詹文龙)[4]

[1]*Department of Nuclear Physics, China Institute of Atomic Energy, Beijing 102413, China*
[2]*Shanghai Institute of Applied Physics, Chinese Academy of Sciences, Shanghai 201800, China*
[3]*College of Physics and Technology, Guangxi Normal University, Guilin 541004, China*
[4]*Institute of Modern Physics, Chinese Academy of Sciences, Lanzhou 730000, China*
[5]*State Key Laboratory of Nuclear Physics and Technology, School of Physics, Peking University, Beijing 100871, China*

The β decay of the drip-line nucleus ^{20}Mg gives important information on key astrophysical resonances in ^{20}Na, which are relevant to the onset of the rapid proton capture process. A detailed β-decay spectroscopic study of ^{20}Mg was performed by a continuous-implantation method. A detection system was specially developed for charged-particle decay studies, giving improved spectroscopic information including the delayed proton energies, the half-life of ^{20}Mg, the excitation energies, the branching ratios, and the log ft values for the states in ^{20}Na populated in the β decay of ^{20}Mg. A new proton branch was observed and the corresponding excited state in ^{20}Na was proposed. The large isospin asymmetry for the mirror decays of ^{20}Mg and ^{20}O was also well reproduced. To resolve the long-standing problem about the astrophysically interesting 2645 keV resonance in ^{20}Na convincingly, a higher-statistics measurement may still be needed.

I. INTRODUCTION

Information about short-lived nuclei is essential to resolve some of the long-standing mysteries of the astrophysical rapid proton capture process (rp process) [1], namely, the main astronomical site and its mechanism. β decay can be a good way to study some specific resonances in the daughter nucleus under some stellar environments, for example, to determine the spin and parity of the resonances populated in the β decay on the basis of the selection rules. A large number of decay channels including β-delayed particle emission will open due to the high β-decay energy and low separation energy of nucleons for nuclides adjacent to the proton drip line. Studies of the β decay and β-delayed particle emission of exotic nuclei also advance our understanding of the nature of the basic interactions which affect the structure of nuclei [2–4].

In explosive hydrogen burning environments such as novae and x-ray bursts, the ^{15}O$(\alpha,\gamma)^{19}$Ne$(p,\gamma)^{20}$Na reaction sequence is a possible breakout path from the hot CNO cycle into the rp process [5,6]. The reaction rate of a (p,γ) or (α,γ) reaction is dependent on resonance energies and resonance strengths. For the ^{19}Ne$(p,\gamma)^{20}$Na reaction, its stellar reaction rate is expected to be dominated by the low-energy resonant levels in ^{20}Na. The nuclear structure information, such as excitation energy, spin, parity, and partial decay width of the states near and just above the proton-separation threshold

in ^{20}Na, plays a key role to estimate the reaction rate. In particular, the first excited state above the threshold was found at ∼2645 keV in ^{20}Na, whereas its property has been controversial for 30 years [7–9]. The resonance energy was well known but only the upper limit of the resonance strength was obtained. A series of experimental and theoretical studies through the ^{20}Ne$(^3$He,$t)^{20}$Na charge exchange reaction [10–19], the ^{20}Ne$(p,\gamma)^{20}$Na reaction with radioactive ^{19}Ne beams via inverse-kinematics method [20–25], shell-model calculations [26,27], and other related studies [28–30] have been conducted. However, the spin and parity assignment of the state is unsettled even after these extensive investigations. The two most likely spin and parity for this state are 1^+ and 3^+. The state can be populated in an allowed transition from ^{20}Mg in the former case while in the latter case the transition will be strongly forbidden [31]. The β decay of ^{20}Mg can be used as an alternative way to investigate the configuration of the 2645 keV state in ^{20}Na.

Apart from the measurement of the decay properties of the resonances populated in the β decay of ^{20}Mg, other motivations for studying the β decay of the lightest bound magnesium isotope, i.e., ^{20}Mg, are to measure the β-decay strength distribution and investigate the quenching of Gamow-Teller strength in β decay, to test the isobaric multiplet mass equation, and to study the isospin symmetry in comparison with the mirror decay and the mirror nucleus [32].

The β-decay study of $T_z = -2$ proton-rich nucleus ^{20}Mg has been performed with various detection methods. The β-delayed protons from ^{20}Mg decay were first observed through helium-jet techniques by Moltz *et al.* [33] in 1979, providing the first test of the validity of the isobaric multiplet

mass equation for the $A = 20$ quintet in spite of the low statistics and the high contamination from ^{20}Na. In 1992, two β-delayed proton spectroscopic studies of ^{20}Mg were performed by Kubono *et al.* [34,35] and Görres *et al.* [36], respectively. Both of them implanted the projectile fragments into silicon detectors and more β-delayed proton peaks from ^{20}Mg decay were observed. Kubono *et al* estimated an upper limit of 1% for the branching ratio to the 2637 keV state in ^{20}Na and assigned this state to be the analog of the 3175 keV 1^+ state in ^{20}F, while Görres *et al.* reduced this upper limit to 0.2%. The most comprehensive β-decay spectroscopy of ^{20}Mg was performed by Piechaczek *et al.* [32] in 1995. Both of the protons and γ rays were measured, from which an improved decay scheme of ^{20}Mg was constructed. An upper limit of 0.1% for the branching ratio to the 2645 keV state was determined as well. Recently, in 2012, Wallace *et al.* [31] performed a β-delayed proton spectroscopic study by implanting ions into a very thin double-sided silicon strip detector. They reported a more stringent upper limit on the branching ratio to the 2647 keV state of 0.02% with a 90% confidence level, which strongly supported a 3^+ assignment, being the analog of the 2966 keV 3^+ state in ^{20}F. A breakdown of the isobaric multiplet mass equation in the $A = 20, T = 2$ quintet was reported by Gallant *et al.* [37]. Soon in 2015, the latest β-decay study of ^{20}Mg was done by Glassman *et al.* [38]. They measured the β-delayed γ rays from ^{20}Mg decay and determined the excitation energy of the lowest $T = 2$ state in ^{20}Na with high precision. The isobaric multiplet mass equation for the $A = 20$ quintet was found to be revalidated.

It is a serious challenge to assign the proton peaks to the right decay branches and reconstruct the decay scheme, as numerous states in ^{20}Na and the proton daughter nucleus ^{19}Ne are populated in the β decay of ^{20}Mg [32]. In the present paper, we report the detailed information about the complicated decay of ^{20}Mg obtained by measuring the emitted particles and γ rays in the β decay with high efficiency and high resolution. For the sake of completeness, the results of an experiment [39,40] performed a few months after the present experiment are also included in this paper.

II. EXPERIMENTAL TECHNIQUES

The experiment was performed at the Heavy Ion Research Facility of Lanzhou (HIRFL) [41] in December 2014. A ^{28}Si primary beam at 75.8 MeV/nucleon with an intensity of $\sim$37 e nA ($\sim$2.6 p nA) impinged on a 1500 μm thick ^{9}Be target. The main setting of the Radioactive Ion Beam Line in Lanzhou (RIBLL) [42] for the selection of the secondary beam was optimized on ^{22}Si, and the relevant results will be published elsewhere [43]. As shown in Fig. 1, the ions in the secondary beam were identified by energy-loss (ΔE) and time of flight (ToF) with respect to the two focus planes of RIBLL given by silicon detectors and two scintillation detectors, respectively. In the secondary beam, the accompanying ^{20}Mg ions were provided with an average intensity of 0.59 particles per second and an average purity of 0.13%. In order to develop an advanced detection system with high detection efficiency and low detection threshold for charged particle in the decay, several technologies and solutions were conceived
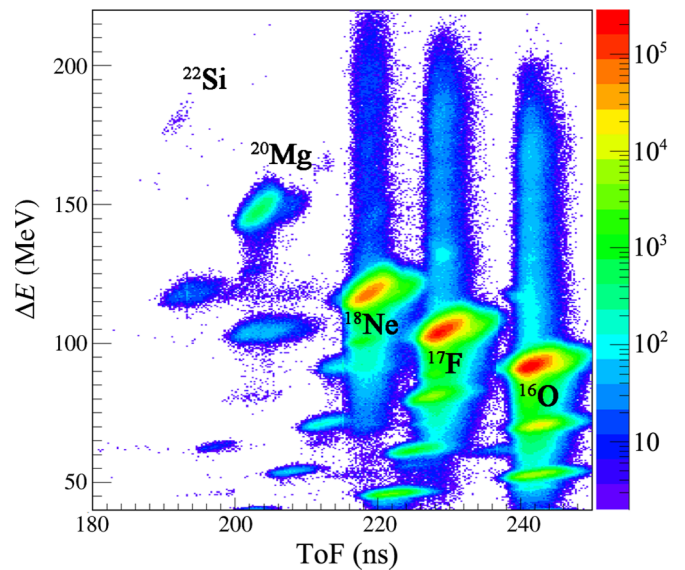

FIG. 1. Two-dimensional identification plot of ΔE and ToF.

and implemented on the bases of our previous experimental methods [44–48]. Details concerning the detection setup were described in Refs. [49,50], and here we give only the main features. The isotopes of interest were implanted into two double-sided silicon strip detectors (DSSD1 of 149 μm thickness and DSSD2 of 66 μm thickness), which also served as the subsequent decay detectors. A 314 μm thick quadrant silicon detector [51] (QSD1) was mounted downstream to serve as an anticoincidence of the penetrating heavy ions and also to detect the charged particles escaping from DSSD2. A 1546 μm thick QSD2 was installed downstream to detect the β particles. QSD3 and QSD4, each with a thickness of $\sim$300 μm, were installed at the end to suppress the possible disturbances from the penetrating light particles (^{1}H, ^{2}H, ^{3}H, and ^{4}He) coming along with the beam. Besides, the silicon detectors were surrounded by five clover-type high-purity germanium (HPGe) detectors, which were employed to measure the γ rays. In front of the silicon detectors array, an aluminum degrader was installed to adjust the stopping range of the ions in the DSSDs. During the experiment, the total numbers of ^{20}Mg ions implanted into DSSD1 and DSSD2 were determined to be 2.0×10^5 and 1.2×10^5, respectively. The known β-delayed protons from ^{21}Mg decay [52] measured in the previous stage of the experiment were used for the energy calibrations of the DSSDs. The known β-delayed γ rays from ^{22}Mg decay [53,54] and ^{24}Si decay [55] measured in the latter stage of the experiment were used for the absolute efficiency calibrations of the clover detectors. The clover detectors were also calibrated in energy and intrinsic efficiency with a ^{152}Eu standard source.

III. RESULTS

The total β-delayed particle spectrum from ^{20}Mg decay measured by the two DSSDs is presented in Fig. 2. The time difference between an implantation event and all the subsequent decay events was limited within five half-life
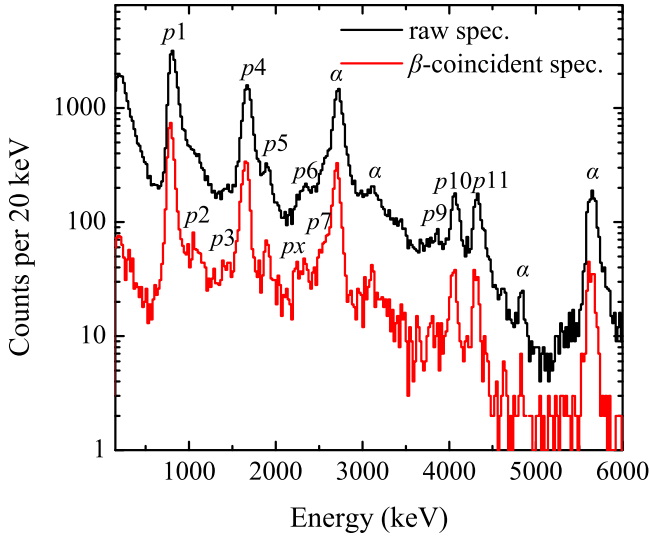
FIG. 2. β-delayed particle spectra from ^{20}Mg decay measured by the two DSSDs. The red curve represents the β-coincident particle spectrum. The proton peaks come from the β-delayed proton decay of ^{20}Mg are labeled with p followed by a number, and the α peaks come from the β-delayed α decay of ^{20}Na are labeled with letter α.

windows (450 ms). Charged particles escaping from a DSSD will deposit incomplete energies in the DSSD and the residual energies of the escaping charged particles can be measured by the other DSSD with high efficiency. Figure 2 shows the sum of the deposited energy in DSSD1 and DSSD2. The β pile-up effect of the particle spectrum can be reduced by requiring a coincidence with β signals in the QSD2. This condition selects the decay events with short flight paths of β particles

in the DSSDs, hence more proton peaks can be identified in the β-coincident spectrum. As shown in Fig. 2, the β-delayed protons from ^{20}Mg decay are marked with p followed by a number, and the β-delayed α from ^{20}Na decay are marked with letter α. The origin of each particle peak in the spectrum can be identified with a half-life analysis. A new weak peak labeled with px at 2256 keV was observed in the particle spectrum, which was confirmed to be the β-delayed protons from ^{20}Mg decay as its half-life was estimated to be 101.9 ± 14.9 ms. We also investigated several subsets of the data from different strips of the DSSDs at different stages of the beam collection period to exclude the possibility of false signals, which serves as an additional consistency check of the new peak. In a previous measurement [31], a $\sim$2340 keV peak was indicated in the β-delayed particle spectrum from ^{20}Mg decay. It is to be noted that the shape of their $\sim$2340 keV peak is much broader than those of other peaks, while the relatively better resolution and higher sensitivity achieved in the present work made it possible to clearly distinguish the two peaks unresolved in their $\sim$2340 keV peak. The proton-decay branching ratios can be calculated by counting the β-delayed proton-decay events in the particle spectrum, divided by the numbers of the implanted ^{20}Mg ions. The background subtraction of the proton numbers, the proton detection efficiency correction of the DSSDs, and the dead-time correction of the data acquisition system should be applied, as well. The energies and the branching ratios for the β-delayed protons from ^{20}Mg decay observed in the present work are summarized in Table I, and the agreement with the literature values is good within the error for all the proton groups. The errors for energies are attributed to the uncertainties of the calibration parameters and the Gaussian fitting uncertainties of the peak-energies. The errors for branching ratios include the statistical errors

TABLE I. Decay energies (E_p) and branching ratios (br) for β-delayed protons from ^{20}Mg decay.

Proton[a]	Kubono [35]		Görres [36]		Piechaczek [32]		Wallace [31]		Lund [39]	Present Work	
	E_p (keV)	br (%)	E_p (keV)	br (%)	E_p (keV)	br (%)	E_p (keV)	br (%)	E_p (keV)	E_p (keV)	br (%)
$p1$	847	9	807(10)	10.7(5)	806(2)	11.5(14)	797(2)		780(8)	808(13)	8.6(7)
							885(15)	0.5(1)			
$p2$					1056(30)	0.7(1)	$\sim$1050			1071(18)	0.7(2)
$p3$					1441(30)					1416(18)	0.4(1)
$p4$	1669	5	1670(10)	5.4(5)	1679(15)	4.8(6)	1670(10)		1656(10)	1673(14)	5.6(5)
$p5$	1891				1928(16)	1.1(2)	1903(5)		1907(3)	1897(17)	1.1(1)
									2138(6)		
px										2256(18)	0.3(1)
$p6$	2351				2344(25)	0.3(1)+0.8(1)	$\sim$2340		2335(3)	2359(18)	0.4(1)
$p7$					2559(45)				2567(4)	2576(20)	0.2(1)
$p8$	2865				2884(45)				2768(6)		
									3081(12)		
									3320(6)		
$p9$					3837(35)	0.2(1)+0.1(1)			3817(3)	3853(17)	0.3(1)
$p10$	3990	0.8	4098(19)	1.3(6)	4071(30)	0.7(1)+0.59(1)+0.32(1)	$\sim$4080		4051(2)	4076(16)	0.9(1)
$p11$	4239	0.7	4332(16)	1.7(6)	4326(30)	1.8(3)	4332(16)		4303(4)	4337(16)	1.0(1)
									4544(25)		
									4993(16)		

[a]The label numbers of proton peaks correspond to the label numbers in Fig. 2 as well as those in Ref. [32].
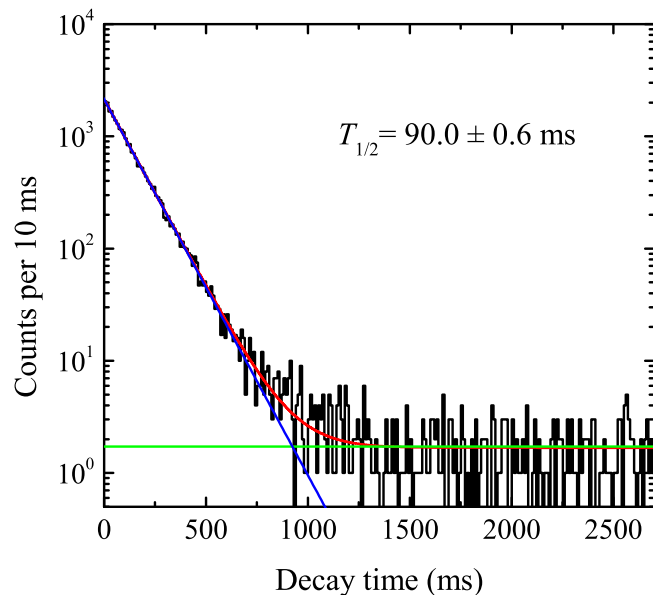
FIG. 3. Decay-time spectrum of ^{20}Mg. The spectrum is fitted with a formula (red line) which can be decoupled into an exponential decay component (blue line) and a constant background component (green line).

and the uncertainties from the background subtraction, the detection efficiency correction, and the dead-time correction.

As shown in Fig. 3, the decay-time spectrum of ^{20}Mg is generated by the summation of the time difference between an implantation event and all the subsequent decay events which occurs in the same x-y pixel of the DSSD. In order to eliminate the influence of the β-delayed α decay of ^{20}Na (the daughter of ^{20}Mg β decay), only the two strongest proton peaks ($p1$ and $p4$) are taken into account. The decay-time spectrum contains a small quantity of random correlations, in which the implantation events could be accidentally correlated with decay events from other implantation events or disturbance events from background. All the true correlated implantation and decay event pairs generate an exponential curve whereas all the uncorrelated event pairs yield a constant background. In Fig. 3, a fit with a function composed of an exponential decay and a constant background yields the half-life of ^{20}Mg to be 90.0 ± 0.6 ms. The uncertainty is derived from the fitting program. The $\chi^2/\text{NDF} = 1.14$ represents a good fit based
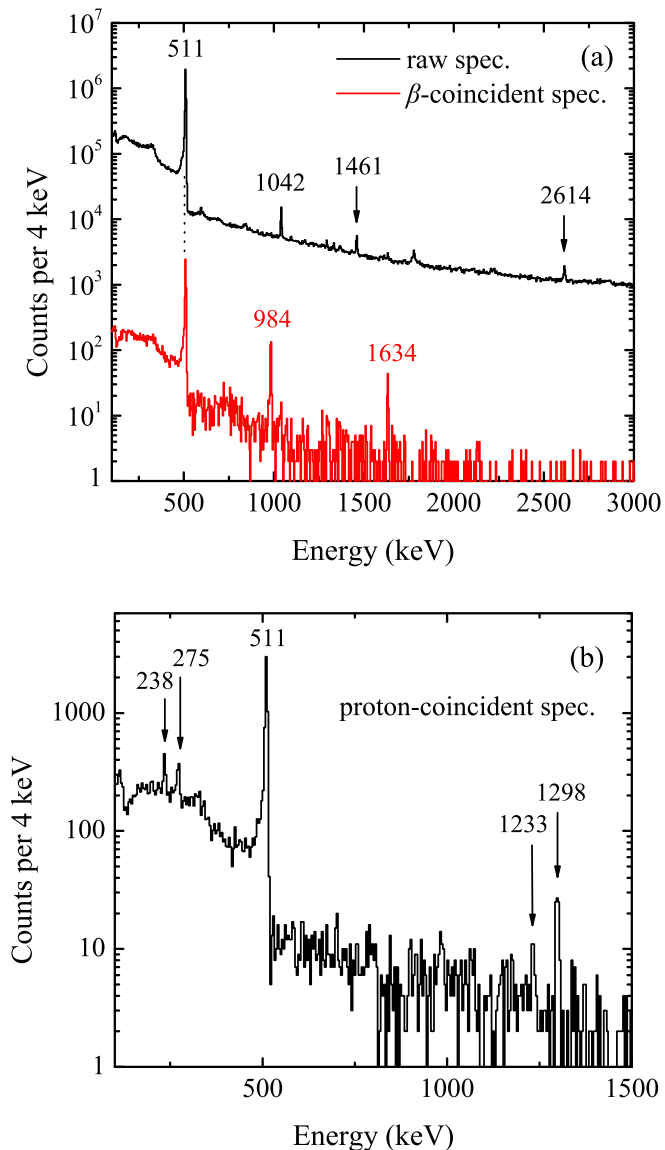
TABLE II. Half-lives of ^{20}Mg.

Literature	Year	$T_{1/2}$ (ms)
Moltz [33]	1979	95^{+80}_{-50}
Kubono [35]	1992	114 ± 17
Görres [36]	1992	82 ± 4
Piechaczek [32]	1995	95 ± 3
Shell-model calculation [32]	1995	101.8
Wallace [31]	2012	~ 90
Lund [40]	2016	91.4 ± 1.0
Present work	2016	90.0 ± 0.6

FIG. 4. γ-ray spectra measured by the clover detectors. (a) The raw γ-ray spectrum without any coincidence and the γ-ray spectrum in coincidence with β particles from ^{20}Mg decay. (b) The γ-ray spectrum in coincidence with charged particles from ^{20}Mg decay.

on Ref. [56], where "NDF" refers to the number of degrees of freedom. The result is tabulated and compared with the literature values in Table II, and nice agreement is obtained.

Figure 4(a) shows the raw γ-ray spectrum without any coincidence and the γ-ray spectrum in coincidence with β particles from ^{20}Mg decay. Figure 4(b) shows the γ-ray spectrum with coincidence gating condition on charged particles from ^{20}Mg decay. According to the γ-ray measurements of ^{20}Mg decay conducted by Piechaczek *et al.* at GANIL [32] and recently by Glassman *et al.* at NSCL [38], the interpretations of each γ lines are offered as follows. In Fig. 4(a), the 984 keV γ ray comes from the β-delayed γ decay of ^{20}Mg, and the 1634 keV γ ray comes from the β-delayed γ decay of the daughter nucleus ^{20}Na. The 1042 keV γ ray comes from the β-delayed γ

FIG. 5. γ-ray spectrum in coincidence with $p4$ from ^{20}Mg decay measured by the two DSSDs.

TABLE III. Decay branches contained in each proton peak and the corresponding initial states in ^{20}Na and the final states in ^{19}Ne.

Proton peak	^{20}Na level $\rightarrow$ ^{19}Ne level (keV)
$p1$	$2998 \rightarrow 0$
$p2$	$4801 \rightarrow 1536$
$p3$	$5142 \rightarrow 1536?$
$p4$	$3863 \rightarrow 0, 4130 \rightarrow 275$
$p5$	$4130 \rightarrow 0, 4362 \rightarrow 275?, 5595 \rightarrow 1508$
px	$4721 \rightarrow 275, 5982 \rightarrow 1536?$
$p6$	$4801 \rightarrow 275$
$p7$	$4801 \rightarrow 0$
$p8$	?
$p9$	$6318 \rightarrow 275$
$p10$	$6523 \rightarrow 238, 6523 \rightarrow 275$
$p11$	$6523 \rightarrow 0$

decay of ^{18}Ne, which is a main contaminant in the secondary beam. The 511 keV γ ray comes from the positron-electron annihilation. Besides, there are two γ rays from natural background, i.e., the 1461 keV γ ray from the ^{40}K decay [57] and the 2614 keV γ ray from the ^{208}Tl decay [58]. The β-decay branching ratio to the 984 keV state of ^{20}Na was estimated to be 66.9(46)% by using the counts of the 984 keV γ ray. This value agrees fairly well with the literature value of 69.7(12)% [32]. In Fig. 4(b), the 238, 275, 1233, and 1298 keV γ lines correspond to the deexcitations from the four lowest excited states in ^{19}Ne after proton emissions from the states in ^{20}Na, respectively. In order to distinguish individual decay branches contained in each proton peak, it is necessary to conduct a proton-γ-ray ($p\gamma$) coincidence analysis. An example of γ-ray spectrum in coincidence with $p4$ is shown in Fig. 5. The ratio of the efficiency corrected counts of 275 and 1233 keV γ lines to the count of $p4$ can be used to estimate the branching ratio for this decay branch. If none of the four expected γ lines were observed clearly in the proton-coincident γ-ray spectrum, this decay branch should be assigned as a proton emission to the ground state of ^{19}Ne. A classification of the components contained in each proton peak is summarized in Table III, the decay branch is marked with a "?" in the case which only one event is observed in the proton-coincident γ-ray spectrum and therefore more statistics are needed to give a clear identification of these questionable components. The latest proton-separation energy value of ^{20}Na ($S_p(^{20}$Na$) = 2190.1(11)$ keV [59]) is adopted in the determination of the excitation energies of the states in ^{20}Na. With the above information, together with the branching ratios for each proton peak presented in Table I, the corresponding branching ratios for the ^{20}Na states populated in ^{20}Mg decay can be estimated accordingly. Combined with the half-life and excitation energies measured in the present work, as well as the $Q_{EC} = 10626.9(22)$ keV extracted from the latest mass measurements of ^{20}Na [59] and ^{20}Mg [37], the corresponding

log ft values for each ^{20}Na state can be calculated. The results are listed in Tables IV and V, respectively. In general, the reliability of the assignment of the proton emission suffers from the number of counts in the $p\gamma$ coincidence spectra to some extent. The errors of the present branching ratios values are relatively larger than those of the literature values due to the fact that not all the decay branches can be unambiguously identified in the $p\gamma$ coincidence analysis. The low efficiency for the $p\gamma$ coincidence is also responsible for the missing decay branch. As for the isobaric analogue state (IAS) in ^{20}Na, the excitation energy was determined to be 6523(28) keV by using the weighted average energy of the three decay branches corresponding to the proton emissions from the IAS in ^{20}Na to the ground state, 238 keV state, and 275 keV state in ^{19}Ne, respectively, which are shown in Table III. The present excitation energy of the IAS compares fairly well with the literature values of 6533(15) keV [36], 6521(30) keV [32], 6522(16) keV [31], 6498.4(5) keV [38], and 6496(3) keV [40], despite the fact that the errors of values deduced from β-delayed proton measurements are relatively larger compared with the value determined by β-delayed γ-ray measurement. However, it is apparent that the values from the present work and the above three β-delayed proton measurements [31,32,36] are systematically $\sim$20 keV higher than that from the β-delayed γ-ray measurement. The well-known β-delayed proton lines from ^{21}Mg decay and β-delayed γ rays from ^{20}Na decay were used as the calibration sources, respectively, for these two types of experiments. The systematic bias can be associated with the different reference nuclei adopted in energy calibration. As for the 2645 keV state in ^{20}Na, no discernible proton peak around the expected energy of 455 keV can be observed in the particle spectrum presented in Fig. 2, and an upper limit of its branching ratio is estimated to be 0.24(3)%. The 2645 keV state was predicted to have a much larger proton-decay branch than γ-decay branch [29], making it even more unlikely to observe the γ-ray deexcitation from this state with the present experimental sensitivity. In short, the limited statistics of ^{20}Mg would not allow us to further improve the limit value of 0.02% given by Ref. [31].

TABLE IV. Excitation energies and decay branching ratios (br) for the states in ^{20}Na.

Kubono [35]		Görres [36]		Piechaczek [32]		Wallace [31]		Glassman [38]	Lund [40]		Present Work	
E^* (keV)	br (%)	E^* (keV)	br (%)	E^* (keV)	br (%)	E^* (keV)	br (%)	E^* (keV)	E^* (keV)	br (%)	E^* (keV)	br (%)
990	85		74(7)	984.25(10)	69.7(12)				984.10(25)	72.0(25)	983.9(22)	66.9(46)
2637	⩽1	2645	⩽0.2	2645	⩽0.1	2647(3)	⩽0.02				∼2645	⩽0.24
3046	9	3006(10)	10.7(5)	3001(2)	11.5(14)				2970(8)	10.9(3)	2998(13)	8.6(7)
						3075(15)	0.5(1)					
3868	5	3869(11)	5.4(5)	3874(15)	4.8(6)	3860(10)			3846(10)	4.8(4)	3863(14)	3.7(4)
4090				4123(16)	2.7(3)	4093(5)			4094(2)	2.2(3)	4130(22)	2.3(5)
											4721(18)	1.0(7)
				∼4800	⩾1.9	∼4780			4760(4)	3.3(3)	4801(32)	1.2(4)
									5507(10)	1.00(11)		
				∼5600	⩾1.5				5604(5)	0.16(4)	5595(17)	0.7(3)
									5836(13)	0.56(7)		
				6266(30)	1.2(1)	∼6270			6273(7)	2.1(4)	6318(17)	1.6(9)
6440	1.5	6533(15)	3.0(8)	6521(30)	3.3(4)	6522(16)		6498.4(5)	6496(3)	2.2(2)	6523(28)	3.6(6)
				∼6770	⩾0.03				6749(12)	0.59(8)		
				∼6920	⩾0.01							
									7183(16)	0.08(3)		
				∼7440	⩾0.01							

A comparison between the mirror decays of ^{20}Mg and ^{20}O also provides opportunity to investigate the isospin asymmetry. The degree of isospin symmetry breaking can be reflected through the mirror asymmetry parameter $\delta = \frac{\log ft^+}{\log ft^-} - 1$, where the $\log ft^+$ and $\log ft^-$ values are associated with the β^+ decay of ^{20}Mg and the β^- decay of ^{20}O, respectively [39]. According to the compilation [60], $Q_{\beta^-}(^{20}\text{O}) = 3814$ keV, hence only the two energetically accessible low-lying mirror transitions can be taken into consideration. In Table VI, the information of the mirror transitions extracted from the present measurement is summarized, and the large isospin asymmetry observed in the second mirror transitions confirms the results reported in Ref. [32].

IV. CONCLUSION

A detailed study of the β decay of ^{20}Mg was performed by using a detection system for charged-particle decay studies with a continuous-implantation method. A proton–γ-ray coincidence analysis was applied to the identification of β-delayed proton-decay branches of ^{20}Mg, and a new proton branch with an energy of 2256 keV was observed. Improved spectroscopic information on the decay property of ^{20}Mg was deduced. The good agreement between our results with the literature values proves the validity of the analysis method described above in obtaining accurate information about β decay. The isospin asymmetry for the mirror decays of ^{20}Mg and ^{20}O was investigated, as well. It is expected to increase the present

TABLE V. $\log ft$ values for the states in ^{20}Na.

Kubono [35]		Görres [36]		Piechaczek [32]		Wallace [31]		Lund [40]		Present Work	
E^* (keV)	$\log ft$	E^* (keV)	$\log ft$	E^* (keV)	$\log ft$	E^* (keV)	$\log ft$	E^* (keV)	$\log ft$	E^* (keV)	$\log ft$
	3.87		3.70(5)	984.25(10)	3.83(2)			984.10(25)	3.78(3)	983.9(22)	3.80(4)
2637	⩾5.42	2645	⩾5.85	2645	⩾6.24	2647(3)	⩾6.9			∼2645	⩾5.82
3046	4.31	3006(10)	3.99(4)	3001(2)	4.08(6)			2970(8)	4.07(3)	2998(13)	4.15(4)
						3075(15)	5.41(9)				
3868	4.26	3869(11)	3.99(5)	3874(15)	4.17(6)	3860(10)		3846(10)	4.25(8)	3863(14)	4.23(5)
4090				4123(16)	4.33(6)	4093(5)		4094(2)	4.50(14)	4130(22)	4.40(9)
										4721(18)	4.5(3)
				∼4800	⩽4.23	∼4780		4760(4)	4.06(9)	4801(32)	4.36(11)
								5507(10)	4.25(11)		
				∼5600	⩽3.97			5604(5)	5.0(3)	5595(17)	4.24(19)
								5836(13)	4.34(13)		
				6266(30)	3.72(6)	∼6270		6273(7)	3.5(2)	6318(17)	3.48(25)
6440	3.68	6533(15)	3.08(22)	6521(30)	3.13(6)	6522(16)		6496(3)	3.36(9)	6523(28)	3.01(8)
				∼6770	⩽5.01			6749(12)	3.77(14)		
				∼6920	⩽5.39						
								7183(16)	4.3(4)		
				∼7440	⩽4.99						

TABLE VI. Comparison between the transitions in the mirror β decays of ^{20}Mg and ^{20}O.

Transitions	log ft	Ref.	δ
^{20}O $\rightarrow$ ^{20}F 1057 keV	3.740(6)	Alburger [61]	
^{20}Mg $\rightarrow$ ^{20}Na 984.25(10) keV	3.83(2)	Piechaczek [32]	0.024(6)
^{20}Mg $\rightarrow$ ^{20}Na 984.10(25) keV	3.78(3)	Lund [40]	0.011(8)
^{20}Mg $\rightarrow$ ^{20}Na 983.9(22) keV	3.80(4)	Present work	0.016(11)
^{20}O $\rightarrow$ ^{20}F 3488 keV	3.65(6)	Alburger [61]	
^{20}Mg $\rightarrow$ ^{20}Na 3001(2) keV	4.08(6)	Piechaczek [32]	0.12(3)
^{20}Mg $\rightarrow$ ^{20}Na 2970(8) keV	4.07(3)	Lund [40]	0.12(3)
^{20}Mg $\rightarrow$ ^{20}Na 2998(13) keV	4.15(4)	Present work	0.14(3)

statistics by at least one order of magnitude to set a more stringent limit on the branching ratio for the 2645 keV state than the value reported in Ref. [31]. To clarify the remaining problems on the 2645 keV state in ^{20}Na and construct the decay scheme of ^{20}Mg completely, a further experiment with higher γ-ray detection efficiency and improved statistics is highly desirable on the basis of present work.

[1] H. Schatz *et al.*, Phys. Rep. **294**, 167 (1998).
[2] B. Blank *et al.*, Prog. Part. Nucl. Phys. **60**, 403 (2008).
[3] M. J. G. Borge, Phys. Scr. **T152**, 014013 (2013).
[4] M. Pfützner *et al.*, Rev. Mod. Phys. **84**, 567 (2012).
[5] R. K. Wallace *et al.*, Astrophys. J. Suppl. Ser. **45**, 389 (1981).
[6] M. Wiescher *et al.*, J. Phys. G: Nucl. Part. Phys. **25**, R133 (1999).
[7] S. Kubono, Nucl. Phys. A **588**, c305 (1995).
[8] M. Huyse *et al.*, Nucl. Phys. A **588**, c313 (1995).
[9] M. Huyse *et al.*, J. Phys. G: Nucl. Part. Phys. **38**, 024001 (2011).
[10] L. O. Lamm *et al.*, Z. Phys. A **327**, 239 (1987).
[11] L. O. Lamm *et al.*, Nucl. Phys. A **510**, 503 (1990).
[12] S. Kubono *et al.*, Z. Phys. A **331**, 359 (1988).
[13] S. Kubono *et al.*, Astrophys. J. **344**, 460 (1989).
[14] N. M. Clarke *et al.*, J. Phys. G: Nucl. Part. Phys. **16**, 1547 (1990).
[15] N. M. Clarke *et al.*, J. Phys. G: Nucl. Part. Phys. **19**, 1411 (1993).
[16] M. S. Smith *et al.*, Nucl. Phys. A **536**, 333 (1992).
[17] J. Gorres and M. Wiescher, Phys. Rev. C **52**, 412 (1995).
[18] M. A. Hofstee *et al.*, Nucl. Instrum. Methods Phys. Res. B **99**, 346 (1995).
[19] B. D. Anderson, B. Wetmore, A. R. Baldwin, L. A. C. Garcia, D. M. Manley, R. Madey, J. W. Watson, W. M. Zhang, B. A. Brown, C. C. Foster, and Y. Wang, Phys. Rev. C **52**, 2210 (1995).
[20] R. Coszach, T. Delbar, W. Galster, P. Leleux, I. Licot, E. Lienard, P. Lipnik, C. Michotte, A. Ninane, J. Vervier, C. R. Bain, T. Davinson, R. D. Page, A. C. Shotter, P. J. Woods, D. Baye, F. Binon, P. Descouvemont, P. Duhamel, J. Vanhorenbeeck, M. Vincke, P. Decrock, M. Huyse, P. VanDuppen, G. Vancraeynest, and F. C. Barker, Phys. Rev. C **50**, 1695 (1994).
[21] R. D. Page, G. Vancraeynest, A. C. Shotter, M. Huyse, C. R. Bain, F. Binon, R. Coszach, T. Davinson, P. Decrock, T. Delbar, P. Duhamel, M. Gaelens, W. Galster, P. Leleux, I. Licot, E. Lienard, P. Lipnik, C. Michotte, A. Ninane, P. J. Sellin, C. Sukosd, P. VanDuppen, J. Vanhorenbeeck, J. Vervier, M. Wiescher, and P. J. Woods, Phys. Rev. Lett. **73**, 3066 (1994).
[22] C. Michotte *et al.*, Phys. Lett. B **381**, 402 (1996).
[23] G. Vancraeynest *et al.*, Nucl. Phys. A **616**, 107 (1997).
[24] G. Vancraeynest, P. Decrock, M. Gaelens, M. Huyse, P. VanDuppen, C. R. Bain, T. Davinson, R. D. Page, A. C. Shotter, P. J. Woods, F. Binon, P. Duhamel, J. Vanhorenbeeck, R. Coszach, T. Delbar, W. Galster, J. S. Graulich, P. Leleux, E. Lienard, P. Lipnik, C. Michotte, A. Ninane, J. Vervier, H. Herndl, H. Oberhummer, C. Sukosd, and M. Wiescher, Phys. Rev. C **57**, 2711 (1998).
[25] M. Couder, C. Angulo, E. Casarejos, P. Demaret, P. Leleux, and F. Vanderbist, Phys. Rev. C **69**, 022801 (2004).
[26] B. A. Brown, A. E. Champagne, H. T. Fortune, and R. Sherr, Phys. Rev. C **48**, 1456 (1993).
[27] H. T. Fortune, R. Sherr, and B. A. Brown, Phys. Rev. C **61**, 057303 (2000).
[28] J. Gorres, J. Meissner, J. G. Ross, K. W. Scheller, S. Vouzoukas, M. Wiescher, and J. D. Hinnefeld, Phys. Rev. C **50**, R1270 (1994).
[29] D. Seweryniak *et al.*, Phys. Lett. B **590**, 170 (2004).
[30] J. P. Wallace and P. J. Woods, Phys. Rev. C **86**, 068801 (2012).
[31] J. P. Wallace *et al.*, Phys. Lett. B **712**, 59 (2012).
[32] A. Piechaczek *et al.*, Nucl. Phys. A **584**, 509 (1995).
[33] D. M. Moltz, J. Aysto, M. D. Cable, R. D. vonDincklage, R. F. Parry, J. M. Wouters, and J. Cerny, Phys. Rev. Lett. **42**, 43 (1979).
[34] S. Kubono *et al.*, Nucl. Instrum. Methods Phys. Res. B **70**, 583 (1992).
[35] S. Kubono, N. Ikeda, Y. Funatsu, M. H. Tanaka, T. Nomura, H. Orihara, S. Kato, M. Ohura, T. Kubo, N. Inabe, A. Yoshida, T. Ichihara, M. Ishihara, I. Tanihata, H. Okuno, T. Nakamura, S. Shimoura, H. Toyokawa, C. C. Yun, H. Ohnuma, K. Ashai, A. Chakrabarti, T. Mukhopadhyay, and T. Kajino, Phys. Rev. C **46**, 361 (1992).
[36] J. Gorres, M. Wiescher, K. Scheller, D. J. Morrissey, B. M. Sherrill, D. Bazin, and J. A. Winger, Phys. Rev. C **46**, R833(R) (1992).
[37] A. T. Gallant, M. Brodeur, C. Andreoiu, A. Bader, A. Chaudhuri, U. Chowdhury, A. Grossheim, R. Klawitter, A. A. Kwiatkowski, K. G. Leach, A. Lennarz, T. D. Macdonald, B. E. Schultz, J. Lassen, H. Heggen, S. Raeder, A. Teigelhofer, B. A. Brown, A. Magilligan, J. D. Holt, J. Menendez, J. Simonis, A. Schwenk, and J. Dilling, Phys. Rev. Lett. **113**, 082501 (2014).
[38] B. E. Glassman, D. Perez-Loureiro, C. Wrede, J. Allen, D. W. Bardayan, M. B. Bennett, B. A. Brown, K. A. Chipps,

M. Febbraro, C. Fry, M. R. Hall, O. Hall, S. N. Liddick, P. OMalley, W. Ong, S. D. Pain, S. B. Schwartz, P. Shidling, H. Sims, P. Thompson, and H. Zhang, Phys. Rev. C **92**, 042501(R) (2015).

[39] M. V. Lund, Ph.D. thesis, Aarhus University, 2016.

[40] M. V. Lund *et al.*, Eur. Phys. J. A **52**, 304 (2016).

[41] W. L. Zhan *et al.*, Nucl. Phys. A **805**, 533c (2008).

[42] Z. Y. Sun *et al.*, Nucl. Instrum. Methods Phys. Res. A **503**, 496 (2003).

[43] X. X. Xu *et al.*, Phys. Lett. B (to be published).

[44] L. J. Sun *et al.*, Chin. Phys. Lett. **32**, 012301 (2015).

[45] C. J. Lin, X. X. Xu, H. M. Jia, F. Yang, F. Jia, S. T. Zhang, Z. H. Liu, H. Q. Zhang, H. S. Xu, Z. Y. Sun, J. S. Wang, Z. G. Hu, M. Wang, R. F. Chen, X. Y. Zhang, C. Li, X. G. Lei, Z. G. Xu, G. Q. Xiao, and W. L. Zhan, Phys. Rev. C **80**, 014310 (2009).

[46] X. X. Xu, C. J. Lin, H. M. Jia, F. Yang, F. Jia, Z. D. Wu, S. T. Zhang, Z. H. Liu, H. Q. Zhang, H. S. Xu, Z. Y. Sun, J. S. Wang, Z. G. Hu, M. Wang, R. F. Chen, X. Y. Zhang, C. Li, X. G. Lei, Z. G. Xu, G. Q. Xiao, and W. L. Zhan, Phys. Rev. C **81**, 054317 (2010).

[47] X. X. Xu, C. J. Lin, H. M. Jia, F. Yang, F. Jia, Z. D. Wu, S. T. Zhang, Z. H. Liu, H. Q. Zhang, H. S. Xu, Z. Y. Sun, J. S. Wang, Z. G. Hu, M. Wang, R. F. Chen, X. Y. Zhang, C. Li, X. G. Lei, Z. G. Xu, G. Q. Xiao, and W. L. Zhan, Phys. Rev. C **82**, 064316 (2010).

[48] X. X. Xu *et al.*, Phys. Lett. B **727**, 126 (2013).

[49] L. J. Sun *et al.*, Nucl. Instrum. Methods Phys. Res. A **804**, 1 (2015).

[50] L. J. Sun *et al.*, Nucl. Phys. Rev. **33**, 230 (2016).

[51] P. F. Bao *et al.*, Chin. Phys. C **38**, 126001 (2014).

[52] R. G. Sextro *et al.*, Phys. Rev. C **8**, 258 (1973).

[53] J. C. Hardy, V. E. Iacob, M. Sanchez-Vega, R. G. Neilson, A. Azhari, C. A. Gagliardi, V. E. Mayes, X. Tang, L. Trache, and R. E. Tribble, Phys. Rev. Lett. **91** 082501 (2003).

[54] Y. G. Ma *et al.*, Phys. Lett. B **743**, 306 (2015).

[55] Y. Ichikawa, T. K. Onishi, D. Suzuki, H. Iwasaki, T. Kubo, V. Naik, A. Chakrabarti, N. Aoi, B. A. Brown, N. Fukuda, S. Kubono, T. Motobayashi, T. Nakabayashi, T. Nakamura, T. Nakao, T. Okumura, H. J. Ong, H. Suzuki, M. K. Suzuki, T. Teranishi, K. N. Yamada, H. Yamaguchi, and H. Sakurai, Phys. Rev. C **80**, 044302 (2009).

[56] U. C. Bergmann *et al.*, Nucl. Phys. A **701**, 213 (2002).

[57] J. A. Cameron *et al.*, Nucl. Data Sheets **102**, 293 (2004).

[58] M. J. Martin *et al.*, Nucl. Data Sheets **108**, 1583 (2007).

[59] C. Wrede, J. A. Clark, C. M. Deibel, T. Faestermann, R. Hertenberger, A. Parikh, H. F. Wirth, S. Bishop, A. A. Chen, K. Eppinger, A. Garcia, R. Krucken, O. Lepyoshkina, G. Rugel, and K. Setoodehnia, Phys. Rev. C **81**, 055503 (2010).

[60] D. R. Tilley *et al.*, Nucl. Phys. A **636**, 249 (1998).

[61] D. E. Alburger, G. Wang, and E. K. Warburton, Phys. Rev. C **35**, 1479 (1987).